Research Article

Survey on H∞ Robust Control of the Solid Oxide Fuel Cell

Haibo Huo [iD],[1,2] Haidong Yang,[1] Kui Xu,[1] Xinghong Kuang,[1,2] and Jingxiang Xu[1,2]

[1]*College of Engineering Science and Technology, Shanghai Ocean University, Shanghai 201306, China*
[2]*Shanghai Engineering Research Center of Marine Renewable Energy, Shanghai 201306, China*

Correspondence should be addressed to Haibo Huo; hbhuo@shou.edu.cn

Excessive use of fuel or being underutilized will make the actual performance of solid oxide fuel cells (SOFCs) affected by a lot, and at the same time, in order to meet the demands of DC load voltage, a controller of the SOFC that is subjected to small varying loads is proposed on the basis of H_∞ control theory. For the controller design, a state-space representation of the SOFC by using small-signal linearization is derived. To evaluate the control performance, the presented H_∞ controller is tested on the SOFC stack with various load disturbances. The results show that the obtained H_∞ controller can mitigate the voltage oscillations and deviations and can keep fuel utilization constant at varying loads.

1. Introduction

Fuel cells (FCs) have notable potential for power generation in stationary, portable, and transport applications [1]. As one of the most promising types of FC, the solid oxide fuel cell (SOFC) has a high energy conversion efficiency from 60% to 80%. Furthermore, high-quality exhaust energy makes it suitable for distributed generation (DG).

Fuel utilization is the most critical constraint for the SOFC system safety [2]. An overused fuel condition (fuel utilization>0.9), which can lead to fuel starvation and then irreversible decay of the fuel cell, should be strictly avoided. However, it is a great waste under a low fuel utilization when there is no cycling of the anode gas flow, thus causing a low generation efficiency and the increased fuel cost. By far, constant fuel utilization is a primary mode of operation of SOFCs [3, 4]. So, it is essential to design control strategies for transient control of fuel utilization.

The stability of the voltage is very important for the power quality of the converted electricity. In order to mitigate the voltage fluctuation and to improve the load-following capability, different voltage control strategies have been proposed. Moreover, an aggressive control action may cause some potential risks in violating the safety range of the fuel utilization [5, 6].

To control the utilization and the terminal voltage of the SOFC, Li et al. designed two control loops, i.e., the inner current feedback used in the constant fuel utilization control and the PI-type controller for keeping the terminal voltage constant [7]. Huo et al. also designed two control loops to maintain the fuel utilization and the output voltage of the SOFC at their desired values, respectively. In particular, the nonlinear model predictive controller (MPC) based on the Hammerstein model was developed to control the output voltage of the SOFC [8]. However, the utilization and the output voltage cannot be kept constant simultaneously. To solve the above problem, Sendjaja and Kariwala designed a decentralized PI controller as the terminal voltage and the fuel utilization of the SOFC were selected as controlled variables (CVs). Simulation results demonstrated that the proposed decentralized PI controller can closely meet the control objectives of the SOFC [9]. Nevertheless, due to considering the interactions between manipulated variables (MVs) and CVs, a centralized controller has a more optimal and comprehensive nature than a decentralized controller.

So far, different centralized control approaches have been proposed for controlling the output voltage and the fuel utilization of the SOFC. The recent studies have shown that the control of the SOFC is challenging due to its slow

response and tight operation constraints [10]. Thus, the model predictive control (MPC) is the most appropriate approach for centralized control implementation. Wang et al. applied a data-driven predictive control approach via the subspace approach for the SOFC system to solve the above control problem [11]. Bhattacharyya et al. designed a nonlinear model predictive controller (NMPC) to meet the requirement of the multiple input multiple output (MIMO) control of power and the fuel utilization [12]. However, the MPC suffers from several typical drawbacks in practical industrial processes. First, its calculation cost is quite large, and second, it is hard to obtain the stability analysis of the MPC [13–15]. As a result, Sedghisigarchi et al. designed a controller using H_∞ control strategy [16]. The results demonstrated the potential of H_∞ control to achieve fast load following, while satisfying constant utilization of operational constraint. However, the detailed design process of the H_∞ controller was not described, and only the fuel utilization was kept constant.

In this paper, for the controller design, the state-space description of the SOFC based on small-signal linearization is derived for the first time. Then, a robust H_∞ controller for constant fuel utilization and output voltage control of the SOFC is proposed. For this control design, the controlled variables include the fuel utilization and the output voltage of the SOFC, the current is taken as a disturbance, and the fuel and oxygen flow rates are employed as the manipulated variables.

This paper is structured as follows: in Section 2, the nonlinear dynamic physical model of the SOFC is simply introduced, and the description of H_∞ control theory is presented in Section 3, whereas Section 4 focuses on the derivation of an accurate state-space representation of the SOFC and H_∞ control synthesis. Furthermore, the validation of the H_∞ controller and the simulation results are reported. Finally, some conclusions are provided.

2. Nonlinear Dynamic Model of the SOFC

To develop the model-based controller, a nonlinear model proposed in the study by Ault et al. [17] is adopted in this paper. The schematic of the model is shown in Figure 1, and the specifications of the SOFC stack are given in Table 1.

The variables of the SOFC can be classified as controlled variables, manipulated variables, and disturbance variables. In this study, the controlled variables are the output voltage and fuel utilization.

2.1. Output Voltage of the SOFC. Nernst's equation and Ohm's law determine the average voltage magnitude of the fuel cell stack. So, applying Nernst's equation and Ohm's law (taking ohmic losses into account), the output voltage of the SOFC can be modeled as follows:

$$V_{dc} = E - rI, \tag{1}$$

$$E = N_0 E_0 + \frac{N_0 RT}{2F} \ln \frac{p_{H_2} p_{O_2}^{0.5}}{p_{H_2O}}, \tag{2}$$

where

$$p_{H_2}(s) = \frac{1/K_{H_2}}{1 + \tau_{H_2}s}\left(q_{H_2}^{in} - 2K_r I\right),$$

$$p_{O_2}(s) = \frac{1/K_{O_2}}{1 + \tau_{O_2}s}\left(q_{O_2}^{in} - K_r I\right), \tag{3}$$

$$p_{H_2O}(s) = \frac{1/K_{H_2O}}{1 + \tau_{H_2O}s}2K_r I.$$

2.2. Fuel Utilization. Fuel utilization is one of the most important variables affecting the performance of the FC and is defined as

$$u_c = \frac{q_{H_2}^{in} - q_{H_2}^{out}}{q_{H_2}^{in}} = \frac{q_{H_2}^{r}}{q_{H_2}^{in}} = \frac{N_0 I}{2F q_{H_2}^{in}}, \tag{4}$$

where $q_{H_2}^{r}$ is the hydrogen-reacted flow rate. Generally, large variations of fuel utilization can cause uneven voltage and temperature distributions in the SOFC [18]. So, fuel utilization is selected as a controlled variable in this paper.

3. H_∞ Control Theory

Robust control theory has been successfully applied to control system designs that require robustness against possible disturbances such as parameter uncertainties, plant and measurement noises, and external disturbances. During the past two decades, the robust H_∞ control problem has attracted great attention from both the academic and industrial communities [19, 20].

Figure 2 shows a classical block diagram for the H_∞ control problem. In Figure 2, $P(s)$ is a linear time-invariant system, and its state-space description is

$$\dot{x} = A\mathbf{x} + B_1\mathbf{w} + B_2\mathbf{u},$$
$$\mathbf{z}_\infty = C_1\mathbf{x} + D_{11}\mathbf{w} + D_{12}\mathbf{u}, \tag{5}$$
$$\mathbf{y} = C_2\mathbf{x} + D_{21}\mathbf{w} + D_{22}\mathbf{u},$$

where $\mathbf{x}$ denotes the state vector, $\mathbf{u}$ is the control input, $\mathbf{w}$ is an exogenous input vector which includes disturbances, measured noise (not considered here), and tracking signals, $\mathbf{y}$ is the measured output, and $\mathbf{z}_\infty$ is a vector of output to be controlled or minimized.

Assuming (A, B_2) is stabilizable, (C_2, A) is detectable, and $D_{22} = 0$. Define the closed-loop transfer function from $\mathbf{w}$ to $\mathbf{z}_\infty$ for a dynamical output feedback law $\mathbf{u} = K(s)\mathbf{y}$ to be $T_{\mathbf{wz}_\infty}(s)$. The design aim of the H_∞ controller is to ensure that the H_∞ norm of the plant transfer function is bounded within limits, i.e.,

$$\left\|T_{\mathbf{wz}_\infty}(s)\right\| \le \gamma, \tag{6}$$

where γ is a given value defined as guaranteed robust performance.

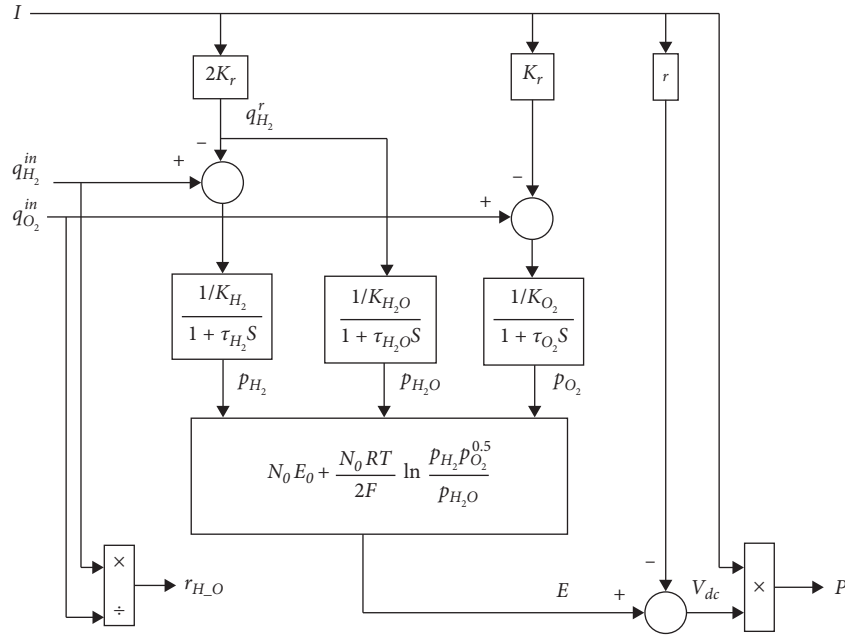We suppose the controller $K(s)$ has the following state-space representation:

Figure 1: Dynamic model of the SOFC stack.

Table 1: Specifications for the SOFC stack.

Symbol	Representation	Value
T	Stack operating temperature	1273 K
N_0	Number of series cells in the stack	384
K_{H_2}	Hydrogen valve molar constant	$0.843 \, \mathrm{mol/(atm \cdot s)}$
K_{H_2O}	Water valve molar constant	$0.281 \, \mathrm{mol/(atm \cdot s)}$
K_{O_2}	Oxygen valve molar constant	$2.52 \, \mathrm{mol/(atm \cdot s)}$
τ_{H_2}	Hydrogen flow response time	26.1 s
τ_{H_2O}	Water flow response time	78.3 s
τ_{O_2}	Oxygen flow response time	2.91 s
E_0	Ideal standard potential (V)	1.18 V
r	Ohmic loss	$0.126 \, \Omega$
r_{H_O}	Ratio of hydrogen to oxygen	1.145
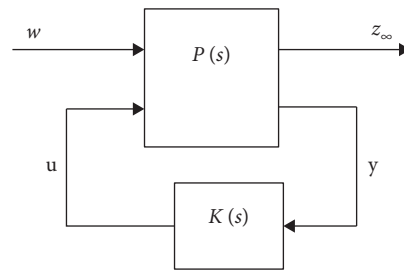
Figure 2: A classical block diagram for the H_∞ control.

$$\dot{\hat{x}} = A_{K\infty}\hat{x} + B_{K\infty}\mathbf{y},$$
$$\mathbf{u} = C_{K\infty}\hat{x} + D_{K\infty}\mathbf{y}, \tag{7}$$

where $\hat{x} \in \mathbf{R}^K$ is the state vector of the controller. Combining equations (5) and (7), we can obtain the closed-loop expression as

$$T_{\mathbf{wz}_\infty}: \begin{bmatrix} \dot{x} \\ \dot{\hat{x}} \\ z \end{bmatrix} = \begin{bmatrix} A + B_2 D_{K\infty} C_2 & B_2 C_{K\infty} & B_1 + B_2 D_{K\infty} D_{21} \\ B_{K\infty} C_2 & A_{K\infty} & B_{K\infty} D_{21} \\ C_1 + D_{12} D_{K\infty} C_2 & D_{12} C_{K\infty} & D_{11} + D_{12} D_{K\infty} D_{21} \end{bmatrix} \begin{bmatrix} \mathbf{x} \\ \hat{x} \\ \mathbf{w} \end{bmatrix}.$$

(8)

Denoting the closed-loop system states $\mathbf{x}_C = \begin{bmatrix} \mathbf{x} \\ \hat{x} \end{bmatrix}$, we can write equation (8) as

$$T_{\mathbf{wz}_\infty}: \begin{bmatrix} \dot{x}_C \\ z \end{bmatrix} = \begin{bmatrix} A_C & B_C \\ C_C & D_C \end{bmatrix} \begin{bmatrix} \mathbf{x}_C \\ \mathbf{w} \end{bmatrix},$$

(9)

where

$$A_C = \begin{bmatrix} A + B_2 D_{K\infty} C_2 & B_2 C_{K\infty} \\ B_{K\infty} C_2 & A_{K\infty} \end{bmatrix},$$

$$B_C = \begin{bmatrix} B_1 + B_2 D_{K\infty} D_{21} \\ B_{K\infty} D_{21} \end{bmatrix},$$

(10)

$$C_C = \begin{bmatrix} C_1 + D_{12} D_{K\infty} C_2 & D_{12} C_{K\infty} \end{bmatrix},$$

$$D_C = \begin{bmatrix} D_{11} + D_{12} D_{K\infty} D_{21} \end{bmatrix}.$$

As a result, the closed-loop transfer function $T_{\mathbf{wz}_\infty}(s)$ can be written as

$$T_{\mathbf{wz}_\infty}(s) = C_C \left(sI - A_C \right)^{-1} B_C + D_C.$$

(11)

4. H$_\infty$ Controller Design for the SOFC

4.1. State-Space Representation of the SOFC. When the working point fluctuates near the stable point within a small scale, the linear control theory is powerful and has been widely used in nonlinear systems [1]. To facilitate the H$_\infty$ controller design, the nonlinear dynamic model of the SOFC is first linearized at its nominal state on the basis of small signal linearization. Because it is impossible to know the load in advance, any load change is treated as a disturbance to the controller [21]. In this study, the SOFC current is taken as a disturbance. Furthermore, the fuel and oxygen flow rates are chosen as the control inputs.

After linearization, the state-space model of the SOFC can be expressed as a function of the state vector $\mathbf{x}(t)$, the control input $q_{H_2}^{in}(t)$, and the disturbance $I(t)$:

$$\Delta \dot{x} = \mathbf{A} \cdot \Delta \mathbf{x} + \mathbf{B}_1 \cdot \Delta I + \mathbf{B}_2 \cdot \Delta q_{H_2}^{in},$$

(12)

where

$$\Delta \mathbf{x} = \begin{bmatrix} \Delta p_{H_2} \\ \Delta p_{H_2O} \\ \Delta p_{O_2} \end{bmatrix},$$

$$A = \begin{bmatrix} -\dfrac{1}{\tau_{H_2}} & 0 & 0 \\ 0 & -\dfrac{1}{\tau_{H_2O}} & 0 \\ 0 & 0 & -\dfrac{1}{\tau_{O_2}} \end{bmatrix},$$

$$B_1 = \begin{bmatrix} -\dfrac{2K_r}{K_{H_2}\tau_{H_2}} \\ \dfrac{2K_r}{K_{H_2O}\tau_{H_2O}} \\ -\dfrac{K_r}{K_{O_2}\tau_{O_2}} \end{bmatrix},$$

(13)

$$B_2 = \begin{bmatrix} \dfrac{1}{K_{H_2}\tau_{H_2}} \\ 0 \\ \dfrac{1}{r_{H\_O}K_{O_2}\tau_{O_2}} \end{bmatrix}.$$

Herein, the nominal operating trajectory is denoted by $\mathbf{x}_0(t)$, which corresponds to the nominal input $q_{H_2,0}^{in}(t)$ and $I_0(t)$. So,

$$\Delta x_i = x_i - x_{0i},$$

$$i = H_2, O_2, H_2O.$$

(14)

Furthermore, linearizing equations (1) and (4) results in

$$\mathbf{z}_\infty = C_1 \cdot \Delta \mathbf{x} + D_{11} \cdot \Delta I + D_{12}\Delta q_{H_2}^{in},$$

$$\mathbf{y} = C_2 \cdot \Delta \mathbf{x} + D_{21} \cdot \Delta I + D_{22} \cdot \Delta q_{H_2}^{in},$$

(15)

where

$$\mathbf{z}_{\infty} = \begin{bmatrix} \Delta V_{dc} \\ \Delta u_c \end{bmatrix}, \tag{16}$$

$$y = \Delta V_{dc}, \tag{17}$$

$$C_1 = \begin{bmatrix} \dfrac{\partial V_{dc}}{\partial p_{H_2}} & \dfrac{\partial V_{dc}}{\partial p_{H_2O}} & \dfrac{\partial V_{dc}}{\partial p_{O_2}} \\ \dfrac{\partial u_c}{\partial p_{H_2}} & \dfrac{\partial u_c}{\partial p_{H_2O}} & \dfrac{\partial u_c}{\partial p_{O_2}} \end{bmatrix}\bigg|_{\mathbf{x}_0, I_0, q_{H_2,0}^{in}}, \tag{18}$$

$$D_{11} = \begin{bmatrix} \dfrac{\partial V_{dc}}{\partial I} \\ \dfrac{\partial u_c}{\partial I} \end{bmatrix}\bigg|_{\mathbf{x}_0, I_0, q_{H_2,0}^{in}}, \tag{19}$$

$$D_{12} = \begin{bmatrix} \dfrac{\partial V_{dc}}{\partial q_{H_2}^{in}} \\ \dfrac{\partial u_c}{\partial q_{H_2}^{in}} \end{bmatrix}\bigg|_{\mathbf{x}_0, I_0, q_{H_2,0}^{in}}, \tag{20}$$

$$C_2 = \begin{bmatrix} \dfrac{\partial V_{dc}}{\partial p_{H_2}} & \dfrac{\partial V_{dc}}{\partial p_{H_2O}} & \dfrac{\partial V_{dc}}{\partial p_{O_2}} \end{bmatrix}\bigg|_{\mathbf{x}_0, I_0, q_{H_2,0}^{in}}, \tag{21}$$

$$D_{21} = \dfrac{\partial V_{dc}}{\partial I}\bigg|_{\mathbf{x}_0, I_0, q_{H_2,0}^{in}}, \tag{22}$$

$$D_{22} = \dfrac{\partial V_{dc}}{\partial q_{H_2}^{in}}\bigg|_{\mathbf{x}_0, I_0, q_{H_2,0}^{in}}. \tag{23}$$

Specifically, we have the following formulas:

$$\dfrac{\partial V_{dc}}{\partial p_{H_2}}\bigg|_{x_0, I_0, q_{H_2,0}^{in}} = \dfrac{N_0 RT}{2F p_{H_2,0}},$$

$$\dfrac{\partial V_{dc}}{\partial p_{H_2O}}\bigg|_{\mathbf{x}_0, I_0, q_{H_2,0}^{in}} = -\dfrac{N_0 RT}{2F p_{H_2O,0}},$$

$$\dfrac{\partial V_{dc}}{\partial p_{O_2}}\bigg|_{\mathbf{x}_0, I_0, q_{H_2,0}^{in}} = \dfrac{N_0 RT}{4F p_{O_2,0}},$$

$$\dfrac{\partial V_{dc}}{\partial I}\bigg|_{\mathbf{x}_0, I_0, q_{H_2,0}^{in}} = -r, \tag{24}$$

$$\dfrac{\partial u_c}{\partial I}\bigg|_{\mathbf{x}_0, I_0, q_{H_2,0}^{in}} = \dfrac{N_0}{2F q_{H_2,0}^{in}},$$

$$\dfrac{\partial u_c}{\partial q_{H_2}^{in}}\bigg|_{\mathbf{x}_0, I_0, q_{H_2,0}^{in}} = -\dfrac{N_0 I_0}{2F \left(q_{H_2,0}^{in}\right)^2}.$$

Here, r_{H_O} is the ratio of hydrogen to oxygen. In general, excess oxygen is expected to make sure that hydrogen reacts with oxygen more completely. In our study, r_{H_O} is held around 1.145, as in [11, 13].

4.2. H_{∞} Control Synthesis and Simulation. Because solver of the linear matrix inequality (LMI) control toolbox is faster and more powerful than classical convex optimization solvers [22], in this study, the H_{∞} controller is synthesized by using the LMI control toolbox. To control the voltage and the fuel utilization of the SOFC, the controlled variables $\mathbf{z}_{\infty}$, as described in equation (16), are chosen to formulate the objectives in an H_{∞} control. In this study, the test system is a 100 kW SOFC connected to a resistive load, and its steady state data are given in Table 2.

Based on the state-space representation of the SOFC in Section 4.1, the H_{∞} control problem can be directly solved by running MATLAB programs. As a result, the optimal H_{∞} performance $\gamma_{opt} = 0.1262$ is obtained, and corresponding parameters of the designed H_{∞} controller are

$$A_{K\infty} = \begin{bmatrix} -0.0133 & 0.0027 & -0.2422 \\ 0.0201 & -0.2952 & -20.7093 \\ 1.5474 & -62.6332 & -8771.8 \end{bmatrix},$$

$$B_{K\infty} = \begin{bmatrix} -0.0015 \\ -0.0053 \\ 2.9262 \end{bmatrix},$$

$$C_{K\infty} = \begin{bmatrix} 0.0002 \\ 0.2654 \\ 113.8685 \end{bmatrix}, \tag{25}$$

$$D_{K\infty} = -0.0202.$$

Afterwards, the proposed H_{∞} controller is tested with various load disturbances by simulation in order to evaluate its performance.

4.2.1. Case 1. To evaluate the control performance of the proposed control strategy, we choose the current disturbance as a multiple step signal which reduces from 372.5 A to 342.5 A at 200 s and goes back to 372.5 A after 650 s, and the profile related to the current is shown in Figure 3. Under this circumstance, the control effect of the output voltage and the fuel utilization of the SOFC are depicted in Figures 4 and 5.

When the load current decreases suddenly, the regulation time of output voltage is 175 s, the maximum overshoot is 0.0044%, the regulation time of fuel utilization is 231 s, and the maximum overshoot is 62.05%. While the load current increases, the regulation time is 173 s and 235 s for the output voltage and the fuel utilization, respectively.

4.2.2. Case 2. Due to power demand variation, multiple step changes occur in the disturbance I, as shown in Figure 6. The current suddenly increases from 372.5 A to 402.5 A at 200 s and goes back to 372.5 A at 650 s. The controlled outputs for the output voltage and the fuel utilization using closed-loop simulations are shown in Figures 7 and 8.

As can be seen from Figures 7 and 8, the proposed H_{∞} controller ensures that the output voltage and the fuel

TABLE 2: Steady state data of the SOFC.

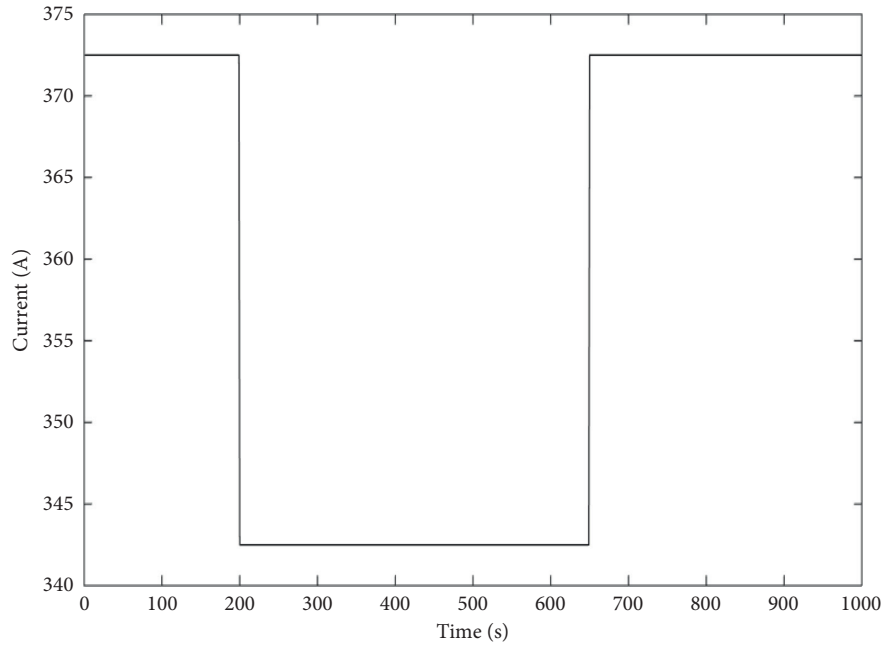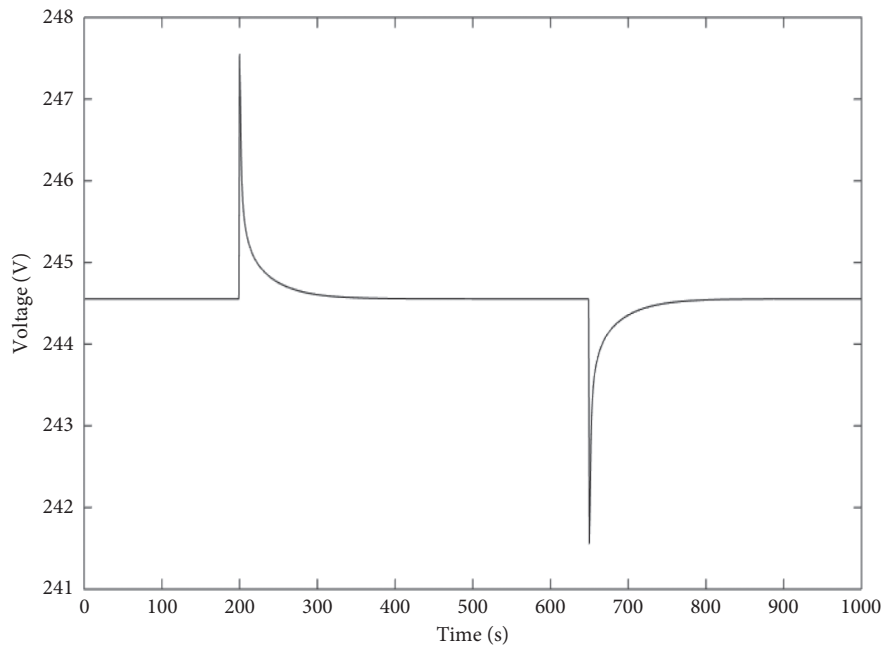| Parameters	Value
$q_{H_2,0}^{in}$	0.95 mol/s
I_0	372.5 A
$V_{dc,0}$	244.55 V
$u_{c,0}$	0.7803
T_0	1273 K

FIGURE 3: The profile of the current for case 1.

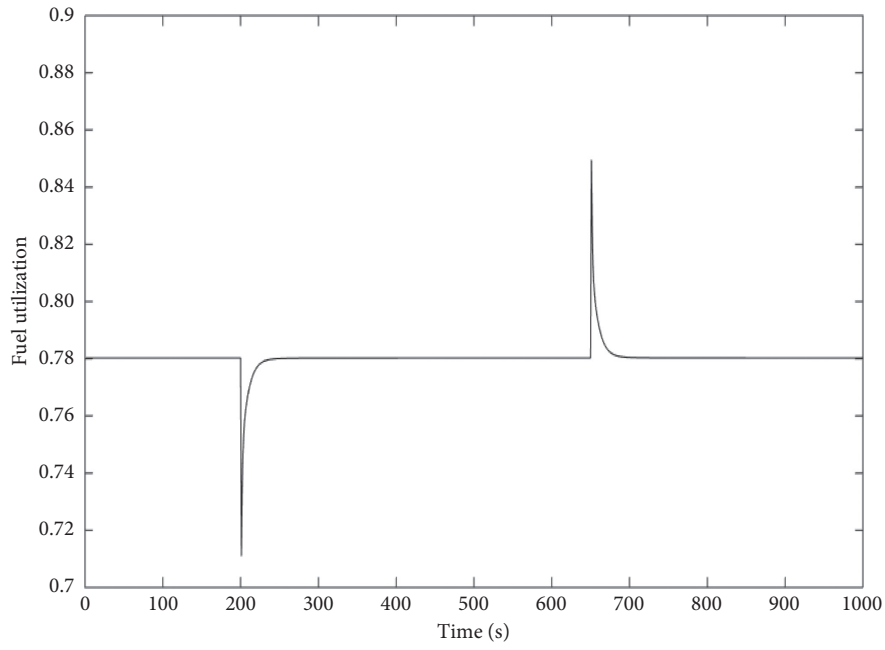FIGURE 4: Voltage control of the SOFC using the H_∞ controller for case 1.

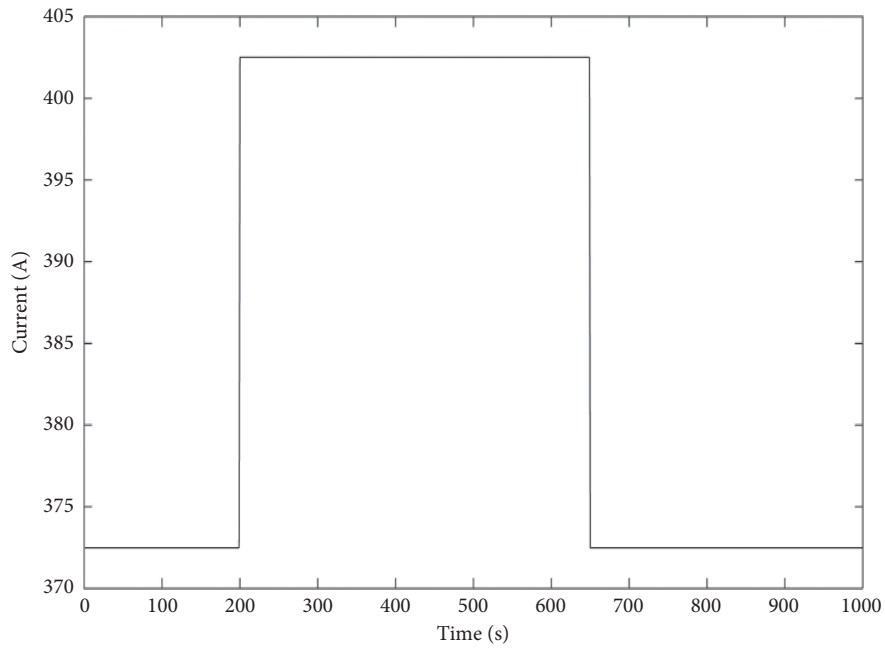Figure 5: Fuel utilization control of the SOFC using the H_∞ controller for case 1.

Figure 6: The profile of the current for case 2.
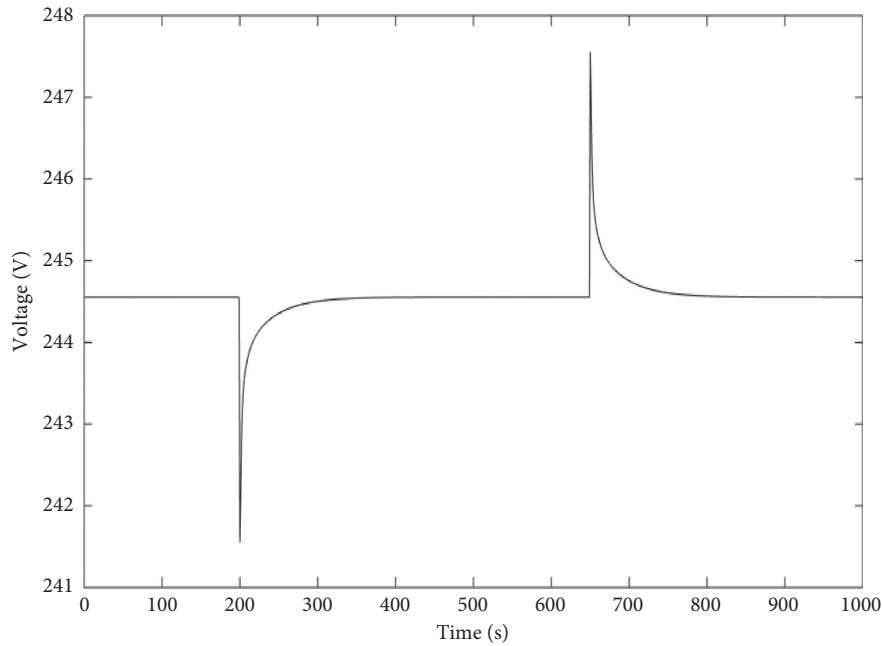
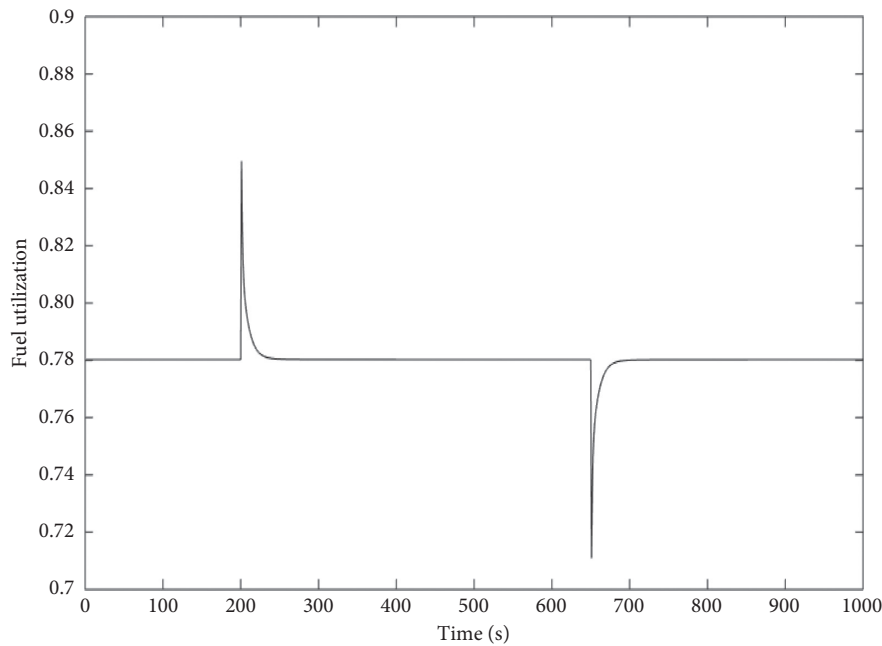FIGURE 7: Voltage control of the SOFC using the H$_\infty$ controller for case 2.

FIGURE 8: Fuel utilization control of the SOFC using the H$_\infty$ controller for case 2.

utilization from the SOFC, respectively, followed their reference values accurately. This clearly demonstrates the excellent performance of the H$_\infty$ controller.

5. Conclusion

To mitigate the voltage oscillations and deviations and keep fuel utilization constant at varying loads, the state-space representation of the SOFC is first derived for the controller design. Then, the H$_\infty$ robust controller for the SOFC is proposed. Simulation results demonstrate its superiority in controlling the output voltage during power requirements' change as well as its capability of controlling fuel utilization for the SOFC system safety.

As a future work, the authors would like to design intelligent control strategies for the SOFC considering temperature variations.

Abbreviations

V_{dc}: Stack output voltage (V)
E: Open-circuit reversible potential (V)

I: Stack current (A)
E_0:   Ideal standard potential (V)
N_0:   Number of series cells in the stack
p_{H_2}:   Hydrogen partial pressure (atm)
p_{O_2}:   Oxygen partial pressure (atm)
p_{H_2O}:   Water vapor partial pressure (atm)
T: Stack operating temperature (K)
F: Faraday's constant (96485 C/mol)
R: Ideal gas constant (8.314 J/(mol K))
K_{H_2}:   Hydrogen valve molar constant (mol/(atm·s))
K_{H_2O}:   Hydrogen valve molar constant (mol/(atm·s))
K_{O_2}:   Oxygen valve molar constant (mol/(atm·s))
τ_{H_2}:   Hydrogen flow response time (s)
τ_{H_2O}:   Water flow response time (s)
τ_{O_2}:   Hydrogen flow response time (s)
$q_{H_2}^{in}$:   Hydrogen input flow (mol/s)
$q_{O_2}^{in}$:   Oxygen input flow (mol/s)
$q_{H_2}^{r}$:   Hydrogen reacted flow (mol/s)
K_r: Constant with the value of $(N_0/4F)$ (mol/(s·A))
u_c: Fuel utilization.

Data Availability

The data (specifications for the SOFC stack) supporting this nonlinear dynamic model of the SOFC are from previously reported studies. These studies are cited at relevant places within this paper as references 17 and 7.

Conflicts of Interest

The authors declare that they have no conflicts of interest.

Acknowledgments

References

[1] B. Cheng, Y. Wang, D. L. Feng, Z. Y. Jiang, and X. X. Zhang, "Macroscopic modeling of solid oxide fuel cell (SOFC) and model-based control of SOFC and gas turbine hybrid system," *Journal of Power Sources*, vol. 66, pp. 83–140, 2018.

[2] S. Han, L. Sun, J. Shen, L. Pan, and K. Lee, "Optimal load-tracking operation of grid-connected solid oxide fuel cells through set point scheduling and combined L1-MPC control," *Energies*, vol. 11, no. 4, pp. 801–823, 2018.

[3] S. Abeysiriwardena and T. Das, "Effect of integral feedback on a class of uncertain nonlinear systems: stability and induced limit cycles," *Journal of Dynamic Systems, Measurement, and Control*, vol. 140, no. 4, 2018.

[4] A. M. Murshed, B. Huang, and K. Nandakumar, "Estimation and control of solid oxide fuel cell system," *Computers & Chemical Engineering*, vol. 34, no. 1, pp. 96–111, 2010.

[5] L. Sun, Q. Hua, J. Shen, Y. Xue, D. Li, and K. Lee, "A combined voltage control strategy for fuel cell," *Sustainability*, vol. 9, no. 9, pp. 1517–1615, 2017.

[6] C. Zhang, Y. He, B. Du, L. Yuan, B. Li, and S. Jiang, "Transformer fault diagnosis method using IoT based monitoring system and ensemble machine learning," *Future Generation Computer Systems*, vol. 108, pp. 533–545, 2020.

[7] Y. H. Li, S. S. Choi, and S. Rajakaruna, "An analysis of the control and operation of a solid oxide fuel-cell power plant in an isolated system," *IEEE Transactions on Energy Conversion*, vol. 20, no. 2, pp. 381–387, 2005.

[8] H.-B. Huo, X.-J. Zhu, W.-Q. Hu, H.-Y. Tu, J. Li, and J. Yang, "Nonlinear model predictive control of SOFC based on a Hammerstein model," *Journal of Power Sources*, vol. 185, no. 1, pp. 338–344, 2008.

[9] A. Y. Sendjaja and V. Kariwala, "Decentralized control of solid oxide fuel cells," *IEEE Transactions on Industrial Informatics*, vol. 7, no. 2, pp. 163–170, 2011.

[10] S. A. Taher and S. Mansouri, "Optimal PI controller design for active power in grid-connected SOFC DG system," *International Journal of Electrical Power & Energy Systems*, vol. 60, pp. 268–274, 2014.

[11] X. Wang, B. Huang, and T. Chen, "Data-driven predictive control for solid oxide fuel cells," *Journal of Process Control*, vol. 17, no. 2, pp. 103–114, 2007.

[12] D. Bhattacharyya and R. Rengaswamy, "System identification and nonlinear model predictive control of a solid oxide fuel cell," *Industrial & Engineering Chemistry Research*, vol. 49, no. 10, pp. 4800–4808, 2010.

[13] T. J. Zhang and G. Feng, "Rapid load following of an SOFC power system via stable fuzzy predictive tracking controller," *IEEE Transactions on Fuzzy Systems*, vol. 17, pp. 357–371, 2009.

[14] M. Lazar, W. P. M. H. Heemels, S. Weiland, and A. Bemporad, "Stabilizing model predictive control of hybrid systems," *IEEE Transactions on Automatic Control*, vol. 51, no. 11, pp. 1813–1818, 2006.

[15] D. Xu, B. Jiang, and P. Shi, "Adaptive observer based data-driven control for nonlinear discrete-time processes," *IEEE Transactions on Automation Science and Engineering*, vol. 11, pp. 1–9, 2014.

[16] K. Sedghisigarchi and A. Feliachi, "H-infinity controller for solid oxide fuel cells," in *Proceedings of 35th IEEE Southeastern Symposium on System Theory*, SSST, Morgantown, WV, USA, March 2003.

[17] J. Padullés, G. W. Ault, and J. R. McDonald, "An integrated SOFC plant dynamic model for power systems simulation," *Journal of Power Sources*, vol. 86, no. 1-2, pp. 495–500, 2000.

[18] C. Stiller, B. Thorud, O. Bolland, R. Kandepu, and L. Imsland, "Control strategy for a solid oxide fuel cell and gas turbine hybrid system," *Journal of Power Sources*, vol. 158, no. 1, pp. 303–315, 2006.

[19] D. Rerkpreedapong, A. Hasanovic, and A. Feliachi, "Robust load frequency control using genetic algorithms and linear matrix inequalities," *IEEE Transactions on Power Systems*, vol. 18, no. 2, pp. 855–861, 2003.

[20] X. H. Chang, *Robust Output Feedback H-Infinity Control and Filtering for Uncertain Linear Systems*pp. 95–124, Springer, Berlin, Heidelberg, Germany, 1st ed. edition, 2014.

[21] R. Kandepu, L. Imsland, B. A. Foss, C. Stiller, B. Thorud, and O. Bolland, "Modeling and control of a SOFC-GT-based autonomous power system," *Energy*, vol. 32, no. 4, pp. 406–417, 2007.

[22] D. Rerkpreedapong and A. Feliachi, "Decentralized H_∞ load frequency control using LMI control toolbox," in *Proceedings of the 2003 IEEE International Symposium on Circuits and Systems*, Bangkok, Thailand, May 2003.